

A Minimalist Model of Single Molecule Spectroscopy in a Dynamic Environment Studied by Metadynamics[†]

Inrok Oh, Eunsang Lee, and YounJoon Jung*

*Department of Chemistry, Seoul National University, Seoul 150-747, Korea. *E-mail: yjjung@snu.ac.kr
Received December 10, 2011, Accepted January 11, 2012*

In this paper we develop a minimalist model of single molecule spectroscopy in a dynamic environment. Our model is based upon a lattice system consisting of a probe molecule embedded in an Ising-model like environment. We assume that the probe molecule interacts with the Ising spins *via* a dipole-dipole potential, and calculate free energy curves and lineshapes of the system. To investigate fluctuation behavior of the system we exploit the metadynamics sampling method. In particular, using the method, we calculate the free energy curve of magnetization of the lattice and that of the transition energy of the probe molecule. Furthermore, we compare efficiencies of three different sampling methods used; unbiased, umbrella, and metadynamics sampling methods. Finally, we explore the lineshape behavior of the probe molecule as the system undergoes a phase transition from a sub-critical and to a super-critical temperature. We show that the transition energy of a probe molecule is broadly distributed due to the heterogeneous, local environments.

Key Words : Single molecule spectroscopy, Lattice model, Dynamic environment, Lineshape, Metadynamics

Introduction

Traditionally spectroscopic measurements in condensed phases have involved a large number of molecules so that ensemble-averaged quantities are usually reported. However, recent developments in optical spectroscopic techniques have allowed us to observe properties of single, individual molecules in various systems,^{1,2} including low temperature crystals,^{3,4} quantum dots,⁵ and biological environments.^{6,7} Those techniques dubbed single molecule spectroscopy (SMS) have made it possible to study properties of molecules at its ultimate detail,⁸ and found unexpected dynamic phenomena at the level of individual molecules, such as spectral diffusion,⁹ power-law blinking processes,^{10,11} and single molecule kinetics,¹² to just name a few.

Single molecule spectroscopy intrinsically eliminates ensemble averaging, and any measurements from SMS report fluctuation phenomena that arise due to either spatial or dynamic (or both) heterogeneity of the interaction between a probe molecule and its local environments. These fluctuation phenomena manifest themselves in many different aspects in SMS. One example is non-trivial, photon counting statistics observed from SMS in various cases. Both experimental^{13,14} and theoretical studies^{11,15-20} have been performed in this area. Another example of the fluctuation phenomena in SMS is dynamic heterogeneity observed in many different systems, including supercooled liquids,²¹⁻²⁴ room-temperature ionic liquids²⁵ as well as protein folding kinetics.^{26,27}

Observing fluctuation phenomena opens up a unique possibility of obtaining rich and valuable microscopic infor-

mation that are normally hidden in ensemble measurements. Much of this information concerns not only a single molecule itself but interaction between the molecule and its local environment. Even though the molecules are chemically identical, they exhibit molecule-to-molecule fluctuations in their spectral properties due to the heterogeneity of local environments. For example, molecules in a cell may behave very differently from those in a solution. Also, spectral lineshapes of probe molecules in matrices can change in time as the solvent configurations undergo dynamical processes. For this reason, it is critical that one has to sample a sufficiently large number of single molecules in SMS in order to observe hidden but important, rare events that are important in dynamics of complex, condensed phase systems. Only by doing so, SMS will provide statistically meaningful properties of molecules as well as dynamic mechanisms in condensed phase systems.

Speaking of the fluctuation phenomena and the importance of rare but important events, similar issues arise in the calculation of free energy surfaces from computer simulations.²⁷⁻²⁹ When sampling equilibrium configurations of the system it is improbable to visit the region of the configuration space with the free energy being sufficiently higher than thermal energy. A chance to visit those regions is exponentially suppressed by the Boltzmann factor. To overcome such difficulty in free energy calculations, novel sampling methods have been invented, including umbrella sampling,³⁰ replica exchange methods,³¹ and non-equilibrium methods³². A recent addition to this list is metadynamics method developed by Parrinello and co-workers.³³ This powerful technique has been applied not only to classical but also to quantum systems.^{34,35}

In this paper we will develop a minimal but generic model of SMS in a condensed-phase environment. Based upon this

[†]This paper is to commemorate Professor Kook Joe Shin's honourable retirement.

model we calculate spectroscopic properties such as magnetization and optical transition energy of the probe molecule *via* the metadynamics method. Thus, the purpose of the paper appears two-fold. First, we will create a minimalist model of SMS. Second, we demonstrate the efficiency of metadynamics method applied to the model and compare the method with other conventional free energy sampling methods.

This paper is organized as follows. First, we develop our model system to be studied in this work. We then give a brief introduction of the metadynamics sampling method in the section of Computational Methods. Then, we present and discuss our calculation results in the next section. Finally, we summarize our results in the Conclusion section.

Model System

Motivation for this work arises from a SMS experiment performed on an impurity molecule embedded in a low-temperature crystal studied by Moerner and co-workers.³⁶ In that study the crystal matrix consisted of *p*-terphenyl molecules with three phenyl rings, and pentacene molecules were introduced as a probe molecule, whose spectral properties are recorded *via* SMS. In the crystal phase, two outer phenyl rings of the *p*-terphenyl molecule lie on the same plane, whereas the central phenyl ring may take one of the two possible orientations with respect to the plane of outer rings. It is known that above a critical temperature the central phenyl ring can take either of two possible configurations with equal probabilities, whereas below the critical temperature, central phenyl rings are ordered in an antiferromagnetic manner because of steric hindrance and anisotropic interactions.

In modeling the system, we regard *p*-terphenyl crystals as a lattice system consisting of interacting two-level systems. One of the simplest ways to describe interactions in two-level systems is *via* Ising model.³⁰ Based upon this idea and following an earlier approach³⁷ we envision the above system as a probe molecule embedded in a two-dimensional Ising model. As well known from statistical mechanics, the Ising model consists of spins on a lattice that interact with other nearest neighbor spins. In our model, spin variables mimic configurations of central phenyl rings in the experiment. With this realization in mind the Hamiltonian of the lattice system is given by that of the Ising model,³⁰

$$H_L = -J \sum_{\langle i,j \rangle} S_i S_j - h \sum_i S_i. \quad (1)$$

Here, S_i is a spin variable at the i -th lattice site with a possible value of either +1 or -1. J and h are a coupling constant and an external magnetic field, respectively. In Eq. (1) the first summation is done over all nearest neighbor pairs while the second is over all spins.

In order to mimic very dilute concentrations of probe molecules in SMS, we introduce a single, probe molecule as a spin variable located at the center of a whole lattice system, denoted by the index 0. To make the situation even

simpler, we assume that the size of the probe molecule is comparable to that of the matrix molecules. Because the molecular weight of the pentacene molecule is larger than that of the *p*-terphenyl molecule, we imagine that the probe molecule is static by fixing the spin configuration of the probe molecule throughout the simulation. It is rather straightforward to lift this assumption and consider the case of a dynamic probe molecule.

The optical transition energy of the probe molecule consists of two terms. The first term is the intrinsic transition energy of a bare probe molecule itself, and is independent of the location of the probe. The other term arises due to the interaction between the probe molecule and time-dependent fluctuations of the environment. We model it *via* dipole-dipole interactions characterized by $1/r^3$. Thus, the transition energy of a probe molecule at the center can be written as

$$H_P = E_0 - J_P \sum_{i \neq 0} \frac{S_i}{r_i^3}, \quad (2)$$

where E_0 is the transition energy of a bare probe molecule and J_P is an energy scale for the interaction between the probe and lattice molecules. r_i is the distance between the probe and the i -th spin in the matrix.

The total Hamiltonian of the system is simply given by

$$H_T = H_L' + H_P = -J \sum_{\langle i,j \rangle, i,j \neq 0} S_i S_j - h \sum_{i \neq 0} S_i - J_P \sum_{i \neq 0} \frac{S_i}{r_i^3} + E_0. \quad (3)$$

Here, the lattice Hamiltonian H_L' is identical to Eq. (1), except that the central site which is occupied by the probe molecule is excluded from the sums. For simplicity, we set the energy scale of our system by choosing $J = J_P = 1$, assuming that the probe-lattice interaction is the same as that between the lattice molecules. We will only consider the case of zero external magnetic field, $h = 0$, as in the experiment.³⁶ Since the bare transition energy E_0 is a constant, independent of the lattice site, we set it to be zero without loss of generality.

Computational Methods: Metadynamics

Suppose we have identified relevant order parameters or collective coordinates of the system over which we want to construct the free energy surfaces. Usually brute-force, unbiased sampling of equilibrium configurations using the Metropolis algorithm is not very efficient in constructing free energy curves, especially when the case when free barriers, much higher than thermal energy, exist in the system. This is indeed the case where two stable phases coexist below the critical temperature in the Ising model.

To overcome this problem, we introduce the metadynamics method.^{33,38} In the metadynamics method, the system Hamiltonian is biased by a history-dependent potential throughout the simulation. Briefly, during the simulation, Gaussian functions are continuously added to the system Hamiltonian. In this way, system will have more chances to explore the configuration space, which otherwise would

have little chances of visitations by the original system. We illustrate the procedure of the metadynamics sampling in the following.

Magnetization. We first calculate the free energy curve of magnetization, $F(m)$, of the two-dimensional Ising system itself without a probe molecule *via* metadynamics. Here, we choose the normalized, spontaneous magnetization m as an order parameter to describe the free energy profile of the system,

$$m = \frac{1}{N} \sum_i S_i. \quad (4)$$

We start with the original Hamiltonian H_L and modify it into a metadynamics Hamiltonian H_k^M ($k = 1, 2, 3, \dots$) through the sequence of metadynamics steps (MDSs) in the following way. For the first MDS, we take the original Hamiltonian H_L as a metadynamics Hamiltonian, H_1^M . Suppose the system is now at the k -th MDS, and the current metadynamics Hamiltonian is given by H_k^M . During the k -th MDS, we perform relatively short, equilibrium samplings of the configurations of the system using H_k^M , and we obtain the probability distribution $P_k(m)$ for a certain range of magnetization. If the probability distribution turns out to be narrow, the system is considered to be in a free energy well. In order to escape from this well, the system needs an energy bias. The energy bias is provided by adding a Gaussian potential to the original Hamiltonian. The Gaussian function $G_k(m)$ to be added to the system at the k -th MDS is given by

$$G_k(m) = A_k \exp\left(-\frac{m - \bar{m}_k^2}{2\delta m_k^2}\right). \quad (5)$$

By adding the Gaussian function G_k to the current metadynamics Hamiltonian H_k^M , we construct a new metadynamics Hamiltonian H_{k+1}^M for the next MDS,

$$H_{k+1}^M = H_k^M + G_k. \quad (6)$$

Using the metadynamics Hamiltonian H_{k+1}^M , we sample the probability distribution, $P_{k+1}(m)$ at the $(k+1)$ -th MDS, and we continue the procedure.

At each MDS, the Gaussian function G_k is constructed from the sampled probability distribution, $P_k(m)$. In Eq. (5), the center of the Gaussian \bar{m}_k is chosen as the most probable value m_{mp}^k in $P_k(m)$. Because most of the probability distributions obtained during one MDS are far from a well-behaved normal distribution, one must be careful in choosing the Gaussian width, δm_k . In practice, we take the width of the Gaussian function δm_k as half of the smaller value between $|m_{\text{max}}^k - m_{\text{mp}}^k|$ and $|m_{\text{min}}^k - m_{\text{mp}}^k|$,

$$\delta m = \frac{1}{2} \min\{|m_{\text{max}}^k - m_{\text{mp}}^k|, |m_{\text{min}}^k - m_{\text{mp}}^k|\}, \quad (7)$$

where m_{max}^k , m_{min}^k , and m_{mp}^k are the maximum, minimum, and most probable magnetization values of $P_k(m)$. A_k is a constant, representing an overall magnitude of the Gaussian. By the time of the k -th MDS, a history dependent potential, $F_k(m)$, will have been constructed by accumulation of

Gaussians and added to the system,

$$F_k(m) = \sum_{l=1}^k G_l(m). \quad (8)$$

Adding Gaussians to the system Hamiltonian plays the role of filling up “puddles” in the free energy curve. Once the Gaussian G_k is added, region of the configuration space with $m \approx \bar{m}_k$ will be avoided in the next sampling, and other regions will have more chance to visit in the next MDSs. By iterating this procedure the system will be able to explore all of the configuration space equally well.

After passing many MDSs, the system will have explored any barriers and wells in the free energy curve, and have sampled the entire range of magnetization sufficiently. Eventually, the free energy curve of the system becomes flattened out. Then, the real free energy curve we want to sample will be obtained as a negative of $F_k(m)$,^{33,38}

$$F(m) = -\lim_{k \rightarrow \infty} F_k(m) \quad (9)$$

Energy of a Probe Molecule. Now, we consider our original model, which consists of a probe molecule embedded in the Ising lattice. The Hamiltonian of the system is given by H_T in Eq. (3). Metadynamics sampling of the probe molecule's energy can be performed in a similar way as that of the magnetization, once we choose the energy of the probe as $E = H_P$ in Eq. (2) as an order parameter. The metadynamics Hamiltonian $H_{T,k}^M$ obtained at the k -th MDS is given by

$$H_{T,k+1}^M = H_T + \sum_{l=1}^k B_l \exp\left(-\frac{(E - \bar{E}_l)^2}{2\delta E_l^2}\right). \quad (10)$$

Here, the Gaussian functions are constructed from the probability distribution of the transition energy of the probe molecule, $P_l(E)$. \bar{E}_l is the mean of the Gaussian and is taken as the most probable energy in $P_l(E)$. There is a technical issue in choosing the width of the Gaussian, δE_l , and we will turn to this later.

Results and Discussion

We use a two-dimensional lattice with the size of 50×50 . We first consider the case of the Ising model itself without a probe molecule, and the Metropolis algorithm is used for performing Monte Carlo simulations. After equilibrating the system, we sample magnetizations at each Monte Carlo step (MCS) during the total 2500 MCSs, which corresponds to one MDS. Then, by following the protocol described in the previous section, we can reconstruct the free energy curve of magnetization.

We first illustrate the performance of metadynamics sampling by showing the trajectory of the Gaussian function added at each MDS. Below the well known critical temperature $T_c = 2.27$, the two-dimensional Ising model exhibits coexistence between two phases, up-spin rich and down-spin rich phases, separated by a large free energy barrier. Thus, it is very difficult to sample both phases in a single simulation

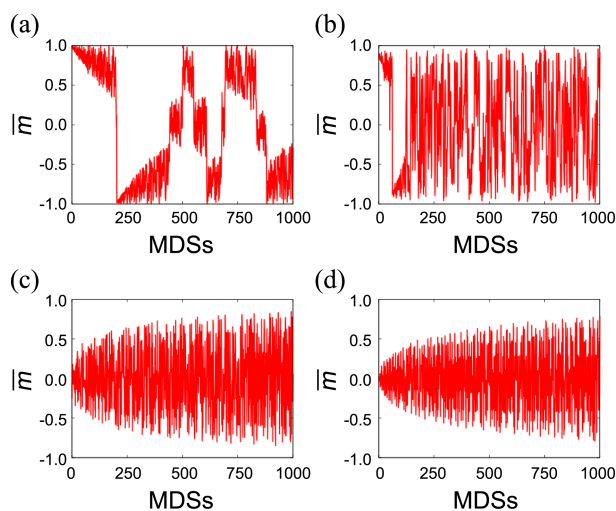


Figure 1. Trajectories of the center of Gaussians added to the system shown at four different temperatures during each MDS. Temperatures are chosen as (a) $T = 1.6$, (b) $T = 2.1$, (c) $T = 2.5$, and (d) $T = 3.0$.

with a usual Metropolis sampling method, especially in the barrier top region. However, the metadynamics sampling method allows a very efficient sampling method as illustrated in Figure 1.

Figure 1 shows trajectories of the center of Gaussian at four different temperatures, $T = 1.6$, 2.1 , 2.5 , and 3.0 , and Figure 1(a) and (b) are subcritical cases, while Figure 1(c) and (d) are supercritical cases, respectively. From wide variations in the average magnetization, it is evident that the metadynamics method allows for an efficient sampling over the entire phase space even below T_c .

Using the metadynamics method it is rather straightforward to calculate the magnetization free energy curve of the system, and we show the result in Figure 2. Figure 2 shows that a high free energy barrier separates two minima, corresponding to ferromagnetic phases at low temperatures below T_c , and a single paramagnetic phase appears at high temperatures above T_c . For the sake of visualization, we arbitrarily shifted the free energy curves such that they coincide at the

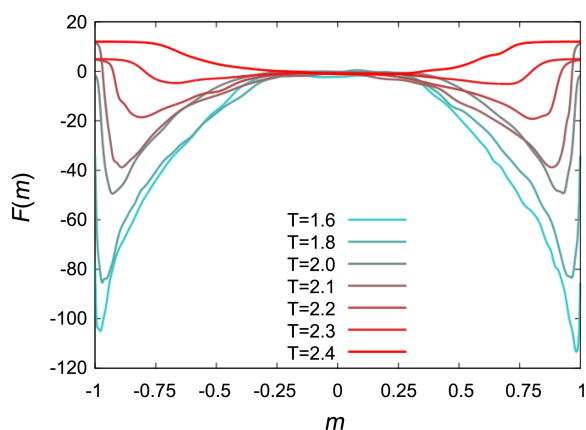


Figure 2. Free energy curves of the magnetization in the two-dimensional Ising model at various temperatures.

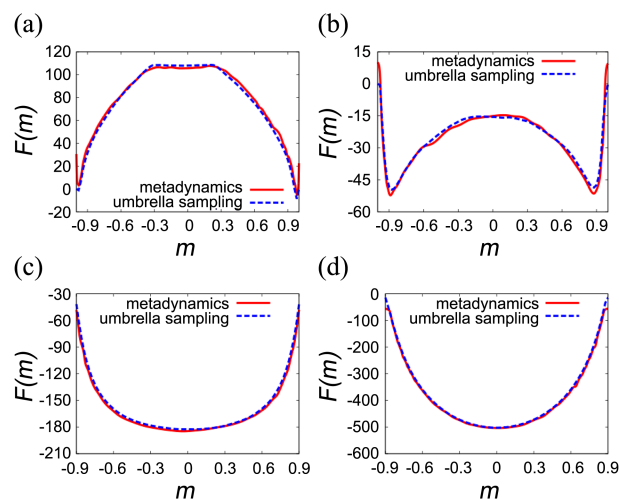


Figure 3. Comparison of free energy curves of the magnetizations sampled with unbiased sampling and with metadynamics method. Temperatures are the same as in Figure 1.

zero magnetization. We notice that there appears a bit of roughness in the calculated free energy curves. This arises because of the finite width of the added Gaussians.

We now check the results obtained from the metadynamics sampling against those from the umbrella sampling³⁹ in Figure 3. In general, they are in good agreements with each other although there are small differences, especially in the low temperature case. We now compare efficiencies of the three methods; unbiased, umbrella, and metadynamics samplings. It turns out that in most cases the metadynamics method is the best. For example, at $T = 2.0$, it only needs about 10^6 MCSs to obtain the free energy curve given in the Figure 3. In contrast, the unbiased sampling requires about 10^{11} MCSs in order to overcome a free energy barrier and to produce a free energy curve with a similar quality of statistics. Comparing with the umbrella sampling method, the metadynamics method turns out to be about 30% faster in the cases we studied.

The unbiased sampling method collects configurations with a usual Boltzmann factor. Since the free energy is given by the logarithm of the probability distribution, a linear increase in the free energy barrier leads to an exponential increase in the number of samplings necessary, which in turn leads to an exponential increase in the simulation time. The umbrella sampling method overcomes this difficulty first by dividing the configuration space according to the order parameter value by applying a biasing potential. In our work, we choose an infinite square well as a biasing potential. Then, each configuration space is sampled one by one, following the Metropolis algorithm. In such a “divide-and-conquer” approach, the umbrella sampling method may result in an $O(N)$ algorithm in favorable situations.

In contrast, the metadynamics method directly estimates the free energy curve by escaping free energy wells successively with the help of added Gaussians. By adding more Gaussians one successively explores higher and higher regions in the free energy curves. Thus, compared with the

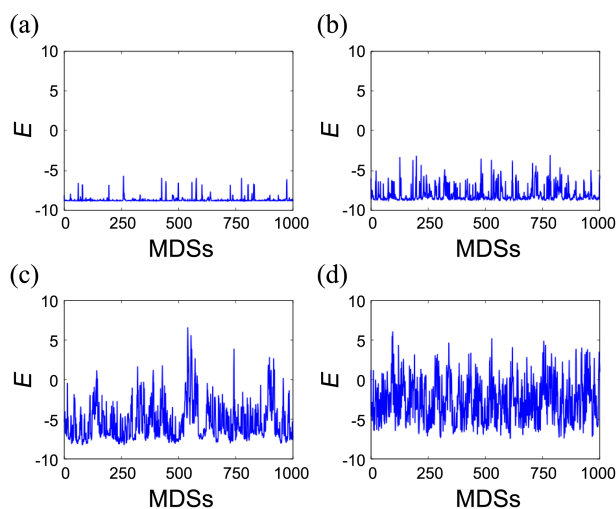


Figure 4. Time-dependent fluctuations of the transition energy of the probe molecule at different temperatures. Temperatures are chosen as (a) $T = 1.6$, (b) $T = 2.1$, (c) $T = 2.5$, and (d) $T = 3.5$.

umbrella sampling the metadynamics method can become very efficient when the free energy curve is steep or has a hierarchical structure. One drawback of the metadynamics method that we already observed is that due to the finite width of the Gaussians it may become difficult to obtain a very smooth free energy curves. Although we did not try to optimize the width of the Gaussians, further optimization will yield lead to an improvement in statistics.

Next, we turn to the case of a probe molecule embedded in the Ising lattice system. Figure 4 shows the transition energy as a function of MCS during the simulation. First, we note that the transition energy constantly fluctuates in time. This is a phenomenon, called spectral diffusion, and it has been observed in many different examples of SMS.^{5,8,9} Our model system, while being very simple, well captures the spectral diffusion behavior observed in SMS. It is also interesting to see that as the temperature is raised the transition energy undergoes a qualitative change, from intermittent to random walk behavior. This indicates that the local environment around the probe molecule is rather static at a low temperature, interrupted by rare fluctuations, and it undergoes a transition into a more fluctuating, dynamic environment as the temperature is raised up.

Since the transition energy is mostly dominated by spins close to the probe molecule due to its inverse-cubic power law, it fluctuates more easily than the magnetization. Accordingly, we sample transition energies at every spin flip during 1 MCS for each MDS. Other conditions of metadynamics are the same as before, except for the area of Gaussians and the method of determining δE . Because of the discreteness of the transition energy, sampling at each MDS may give very narrow distributions of the transition energy. Addition of Gaussians constructed from these distributions thus may not yield efficient sampling method if we choose δE in the same way as δm in Eq. (7). For this reason, we introduce a pre-defined, cut-off value, δE_{cut} . If δE , calculated in the same way as Eq. (7), turns out to be less than δE_{cut} , we take

δE as the latter, otherwise, as the former, that is,

$$\delta E = \max \left\{ \delta E_{\text{cut}}, \frac{1}{2} \min \{ |E_{\text{max}} - E_{\text{mp}}|, |E_{\text{mp}} - E_{\text{min}}| \} \right\}. \quad (11)$$

In this work, we set $\delta E_{\text{cut}} = 0.01$ at $T = 1.6$, $\delta E_{\text{cut}} = 0.02$ at $T = 2.1$, and $\delta E_{\text{cut}} = 0.04$ at both $T = 2.5$ and $T = 3.5$.

Unlike the spontaneous magnetization which involves all spins of the system, the transition energy of the probe molecule is dominated by spins surrounding the probe molecule due to dipolar interaction. Thus, the transition energy may vary quickly compared with the magnetization. Because of that, the unbiased sampling method may be utilized in calculating the free energy profile.

We can check this point by comparing the statistics of unbiased sampling method and that of metadynamics in Figure 5. Figure 5 shows free energy curves obtained by the two methods at four different temperatures. First of all, we note that energies are broadly distributed between -9 and 9 . This wide distribution may seem a little strange at first, especially at a low temperature case. However, by counting contributions of neighboring spins to the transition energy of the probe molecule, it is easy to show that about half of the total transition energy comes from nearest neighbors in the case of dipolar interaction in two-dimension. Thus, thermal fluctuations in local, nearest neighbor spins around the probe will entail rather a broad distribution of the transition energy even below the critical temperature.

Figure 5 also exhibits that the free energy curve is asymmetric, and configurations with low transition energies are more probable than those with high transition energies. As the temperature increases, the free energy curves become less asymmetric. This asymmetry comes from the specific type of the interaction between the probe molecule and the lattice spins given in Eq. (2). In a sense, the probe molecule plays a similar role as an external magnetic field.

As in the case of magnetization, the metadynamics method

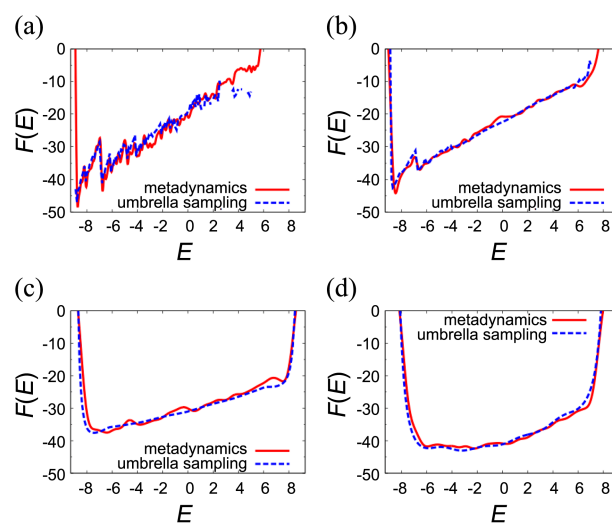


Figure 5. Free energy curves of the transition energy obtained by unbiased sampling and metadynamics sampling methods. Temperatures are the same as in Figure 4.

turns out to be more efficient than the unbiased sampling method in the above calculations. For example, at $T = 1.6$ shown in Figure 5(a), we can only obtain hundreds of configurations with transition energies around $E = 1.0$ even after 640000 MCSs. Thus, the statistics near the high free energy regions, such as $E \approx 6$, is very poor in the unbiased sampling case. Moreover, due to the discrete change in the probe energy the free energy curve is rather rugged. In contrast, the metadynamics method samples well over a whole range of transition energy only over 2000 MCSs. There are some cases where the metadynamics method results in somewhat zigzag-like free energy curves compared with the unbiased sampling methods, for example, in Figure 5(b) and 5(c). Again, this is because the way we choose the width of the Gaussians is rather simple and far from optimal. Further efforts in choosing the width of the Gaussians should be able to resolve this problem.

Finally, in order to mimic the lineshape of a probe molecule observed in SMS, we plot the energy distribution convoluted by a Lorentzian weight function,

$$W(\varepsilon) = \frac{1}{\pi} \int_{-\infty}^{+\infty} dE P(E) \frac{\gamma}{\gamma^2 + (\varepsilon - E)^2}. \quad (12)$$

The function $W(\varepsilon)$ will correspond to the normalized, line-shape function of a probe molecule that is directly measured in SMS. In Eq. (12), the normalized distribution of transition energies is obtained from the free energy curve $F(E)$ sampled by the metadynamics method, and is given by $P(E) = e^{-F(E)}/Z$, where $Z = \int_{-\infty}^{+\infty} dE e^{-F(E)}$. The natural damping constant γ is chosen as $\gamma = 0.1$.

Figure 6 shows calculated the lineshapes of a single probe molecule at different temperatures. At a very low temperature, shown in Figure 6(a), the distribution appears very narrow with small side peaks. This is because spins are strongly correlated with each other, and a probe molecule sees itself located in a rather, static environment. However, as the temperature increases, the lineshape becomes broadened due to time-dependent fluctuations of environments

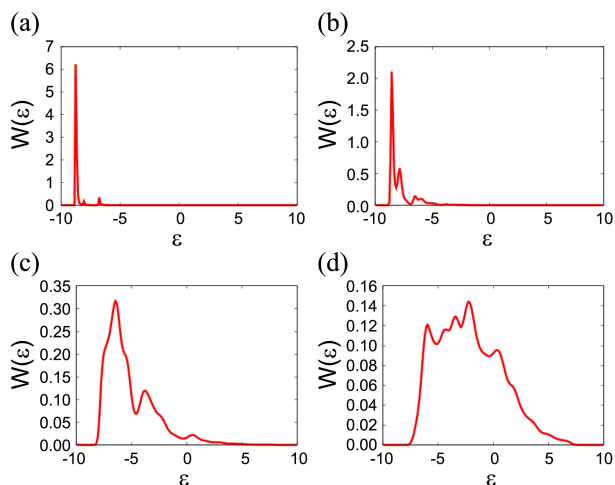


Figure 6. Lineshapes of a probe molecule in our model system of SMS. Temperatures are the same as in Figure 4.

surrounding the probe molecule. At a high temperature, because spins are less correlated, the probe molecule encounters many different realizations of local environments, which results in the spectral broadening. A similar feature has been observed in the case of Ising spin glass system.³⁶

Conclusion

In this paper we have developed a minimalist model of SMS in a dynamic environment. We calculated the free energy profiles of magnetization and transition energy, which are both experimental observables. We also compared efficiencies of different sampling methods. Among the unbiased, umbrella, and metadynamics sampling methods, the metadynamics method turns out to be a very efficient method, particularly when sampling the system with a steep free energy barrier. Although there are some cases where the metadynamics method yields rugged free energy curves, especially in flat regions, it is most efficient in a rough reconstruction of the free energy curve. We also investigate the line broadening phenomena of a probe molecule in an Ising-like environment as the temperature is raised up. Although we have considered a very simple model in this work, the model should be able to serve as a simple, but generic one of SMS in condensed phase environments. We believe that many of the features observed in this study should remain generic.

The current model is arguably the minimalist model for a single molecule spectroscopy in complex environments. Even so, it brings about many interesting features in SMS of condensed phase environments, such as spectral diffusions and line broadenings due to environments. Of course, there are many aspects and details that are missed in this work. For example, in this study we assumed that the probe molecule is static. The probe molecules, however, should be considered time-dependent in general. Also, we have assumed that the interaction strengths between the probe and lattice molecules and that between lattice molecules are the same, and this may not be a good assumption in certain cases. The environmental degrees of freedom can be more complex rather than a simple two-state behavior studied in this work. We will consider these issues as well as others in the future study of SMS in condensed phase environments.

Acknowledgments. This work was supported by the National Research Foundation of Korea (Grant Nos. 2011-0001212, 2011-0003555, and 2011-0018038), the KISTI Supercomputing Center (KCS-2011-C1-07 and KCS-2011-C1-15), and the BK21 Program.

References

1. Basché, T.; Moerner, W. E.; Orrit, M.; Wild, U. P. *Single-Molecule Detection, Imaging, and Spectroscopy*; VCH: New York, 1996.
2. Barkai, E.; Brown, F. L. H.; Orrit, M.; Yang, H. *Theory and Evaluation of Single-Molecule Signals*; World Scientific Press: Singapore, 2008.
3. Moerner, W. E.; Kador, L. *Phys. Rev. Lett.* **1989**, *62*, 2535-2538.

4. Orrit, M.; Bernard, J. *Phys. Rev. Lett.* **1990**, *65*, 2716-2719.
 5. Empedocles, S.; Norris, D.; Bawendi, M. *Phys. Rev. Lett.* **1996**, *77*, 3873-3876.
 6. Xie, X. S.; Trautman, J. K. *Annu. Rev. Phys. Chem.* **1998**, *49*, 441-480.
 7. Weiss, S. *Science* **1999**, *283*, 1676-1683.
 8. Moerner, W. E.; Orrit, M. *Science* **1999**, *283*, 1670-1676.
 9. Zumbusch, A.; Fleury, L.; Brown, R.; Bernard, J.; Orrit, M. *Phys. Rev. Lett.* **1993**, *70*, 3584-3587.
 10. Kuno, M.; Fromm, D. P.; Hamann, H. F.; Gallagher, A.; Nesbitt, D. J. *J. Chem. Phys.* **2000**, *112*, 3117.
 11. Jung, Y.; Barkai, E.; Silbey, R. J. *J. Chem. Phys.* **2002**, *284*, 181-194.
 12. Cao, J.; Silbey, R. J. *J. Phys. Chem. B*, **2008**, *112*, 12867-12880.
 13. Fleury, L.; Segura, J.; Zumofen, G.; Hecht, B.; Wild, U. P. *J. Luminescence* **2001**, *94*, 805-809.
 14. Lounis, B.; Moerner, W. E. *Nature* **2000**, *407*, 491-493.
 15. Jung, Y.; Barkai, E.; Silbey, R. J. *Adv. Chem. Phys.* **2002**, 199-266.
 16. Barkai, E.; Jung, Y.; Silbey, R. *Annu. Rev. Phys. Chem.* **2004**, *55*, 457-507.
 17. Zheng, Y.; Brown, F. L. H. *Phys. Rev. Lett.* **2003**, *90*, 238305.
 18. Mukamel, S. *Phys. Rev. A* **2003**, *68*, 063821.
 19. He, Y.; Barkai, E. *Phys. Rev. Lett.* **2004**, *93*, 068302.
 20. Sung, J.; Silbey, R. J. *J. Chem. Phys. Lett.* **2005**, *415*, 10-14.
 21. Deschenes, L.; Vanden Bout, D. J. *J. Phys. Chem. B* **2002**, *106*, 11438-11445.
 22. Vallée, R.; Cotlet, M.; Hofkens, J.; De Schryver, F. *Macromolecules* **2003**, *36*, 7752-7758.
 23. Jung, Y.; Garrahan, J. P.; Chandler, D. *J. Chem. Phys.* **2005**, *123*, 084509.
 24. Jung, Y.; Garrahan, J. P.; Chandler, D. *Phys. Rev. E* **2004**, *69*, 061205.
 25. Jeong, D.; Choi, M. Y.; Kim, H. J.; Jung, Y. *Phys. Chem. Chem. Phys.* **2010**, *12*, 2001-2010.
 26. Schuler, B.; Eaton, W. A. *Curr. Opin. Struct. Biol.* **2008**, *18*, 16-26.
 27. Lee, E.; Jung, Y. *Bull. Kor. Chem. Soc.* **2011**, *32*, 3051-3056.
 28. Kollman, P. *Chem. Rev.* **1993**, *93*, 2395-2417.
 29. Beveridge, D. L.; DiCapua, F. M. *Annu. Rev. Biophys. Biophys. Chem.* **1989**, *18*, 431-492.
 30. Chandler, D. *Introduction to Modern Statistical Mechanics*; Oxford University Press: New York, USA, 1987.
 31. Sugita, Y.; Okamoto, Y. *Chem. Phys. Lett.* **1999**, *314*, 141-151.
 32. Jarzynski, C. *Phys. Rev. Lett.* **1997**, *78*, 2690-2693.
 33. Laio, A.; Parrinello, M. *Proc. Natl. Acad. Sci. USA* **2002**, *99*, 12562.
 34. Michel, C.; Laio, A.; Mohamed, F.; Krack, M.; Parrinello, M.; Milet, A. *Organometallics* **2007**, *26*, 1241-1249.
 35. Spiwok, V.; Lipovová, P.; Králová, B. *J. Phys. Chem. B* **2007**, *111*, 3073-3076.
 36. Ambrose, W. P.; Moerner, W. E. *Nature* **1991**, *349*, 225-227.
 37. Tanimura, Y.; Takano, H.; Klafter, J. *J. Chem. Phys.* **1998**, *108*, 1851-1858.
 38. Laio, A.; Rodriguez-Fortea, A.; Gervasio, F. L.; Ceccarelli, M.; Parrinello, M. *J. Phys. Chem. B* **2005**, *109*, 6714-6721.
 39. Torrie, G.; Valleau, J. J. *Comput. Phys.* **1977**, *23*, 187-199.
-